## MiR-15b ameliorates SONFH by targeting Smad7 and inhibiting osteogenic differentiation of BMSCs

S.-H. FANG<sup>1</sup>, L. CHEN<sup>2</sup>, H.-H. CHEN<sup>1</sup>, Y.-F. LI<sup>1</sup>, H.-B. LUO<sup>1</sup>, D.-Q. HU<sup>1</sup>, P. CHEN<sup>1</sup>

<sup>1</sup>Department of Orthopedics, The First Affiliated Hospital of Fujian Medical University, Fuzhou, China <sup>2</sup>Department of Anesthesiology, The First Affiliated Hospital of Fujian Medical University, Fuzhou, China

Shanhong Fang and Lu Chen contributed equally to this work

**Abstract.** – OBJECTIVE: The aim of this study was to explore the role of micro ribonucleic acid (miR)-15b in steroid-induced osteonecrosis of the femoral head (SONFH) and its potential mechanism.

PATIENTS AND METHODS: Bone marrow tissues were collected from 5 patients with glucocorticoid (GC)-induced ONFH (GC-ONFH, GC group) and 5 patients with secondary ON-FH (control group) undergoing total hip replacement in our hospital from July 2016 to August 2017. Subsequently, bone marrow mesenchymal stem cells (BMSCs) were separated from bone marrow extracted and cultured in vitro. Quantitative Reverse Transcription-Polymerase Chain Reaction (qRT-PCR) assay was used to detect differentially expressed miRNAs in BMSCs of patients in GC group and control group. BM-SCs were treated with different concentrations of GC. Next, the effect of GC on tmiR-15b expression level was detected via qRT-PCR. Alizarin red staining assay was performed to evaluate the effect of miR-15b on osteogenic differentiation of BMSCs. Meanwhile, the potential targets of miR-15b were predicted using bioinformatics software and validated through luciferase reporter gene assay, respectively. Additionally, Western blotting was conducted to determine the effect of miR-15b on the protein expression of the transforming growth factor beta (TGF-β) signaling pathway.

**RESULTS:** Flow cytometry demonstrated that the proportion of cluster of differentiation 44 (CD44)-positive cells was 99.7%, while that of CD45-positive cells was only 0.17% in cultured BMSCs. This suggested that the purity of BMSCs was relatively high. QRT-PCR assay indicated that the expression level of miR-15b declined significantly in BMSCs of GC group when compared with control group (p<0.01). The osteogenic differentiation capacity of BMSCs was significantly strengthened in GC group compared with control group (p<0.01). Subsequent qRT-PCR assay revealed that GC down-regulated the

expression level of miR-15b in a dose-dependent manner. Besides, the osteogenic differentiation capacity of cells was remarkably strengthened in miR-15b mimic treatment group when compared with control group (p<0.01). Bioinformatics software (TargetScan) predicted that drosophila mothers against decapentaplegic protein 7 (Smad7) might be a potential target of miR-15b, which was indicated by luciferase reporter gene assay. In comparison with control group, miR-15b mimic treatment group exhibited significantly down-regulated protein expression level of Smad7, increased expression level of phosphorylated (p)-Smad2/3 and up-regulated messenger RNA (mRNA) expression level of runt-related transcription factor 2 (Runx2). However, the protein expression level of Smad7 and p-Smad2/3 and the mRNA expression level of Runx2 exhibited opposite trends in miR-15b inhibitor treatment group.

**CONCLUSIONS:** MiR-15b relieves SONFH by targeting Smad7 and repressing osteogenic differentiation of BMSCs.

Key Words:

MiR-15b, Smad7, BMSCs, Osteogenic differentiation, SONFH.

#### Introduction

High-dose steroid hormone is an effective treatment method in clinical practice. It has been widely used for the treatment of many autoimmune diseases and inflammatory diseases, including acute respiratory syndrome, asthma, arthritis, systemic lupus erythematosus, and organ transplantation. However, numerous studies² have verified that the application of steroid hormone in high doses is evidently related to the occurrence of osteonecrosis of the femoral head (ONFH). Kubo et al³

have pointed out that the attack on 51% of 2,200 ONFH patients is associated with the application of steroid hormones. After 2-12 weeks of high-dose steroid hormone therapy, the progression of steroid-induced ONFH (SONFH) may lead to femoral head collapse. This can eventually result in severe hip pain and dysfunction in patients.

At present, relevant pathological mechanisms of SONFH proposed by many scholars<sup>4-7</sup> include the theories of fat embolism, bone cell steatosis and necrosis, intraosseous hypertension and venous stasis, osteoporosis, microvascular injury, intravascular coagulation, and hormone cytotoxicity. Most patients with advanced SONFH eventually require surgery, such as osteotomy, grafting of tibia or total hip replacement. Among all therapeutic regimens for SONFH, bone marrow mesenchymal stem cell (BMSC) transplantation is a good option for the early treatment of ONFH. Sen et al8 have manifested that the therapeutic effect of core decompression combined with BMSC transplantation is remarkably better than that of core decompression alone.

Bone marrow mesenchymal stem cells (BM-SCs) have relatively strong proliferative capacity and multi-lineage differentiation potential. Under certain circumstances, they can be induced to differentiate into osteoblasts, chondroblasts, and adipocytes. Therefore, BMSCs exhibit the potential in the treatment of SONFH<sup>9</sup>. Currently, multiple reports have indicated that BMSCs have enhanced adipose differentiation capacity and weakened osteogenic differentiation ability in a sterol-stimulated environment. Recently, Tan et al<sup>10</sup> have also shown that SONFH may be caused by decreased osteogenic differentiation capacity of BMSCs.

Micro ribonucleic acids (miRNAs) are a class of non-coding RNAs with small molecular weight. They regulate at least 30% of gene expression in cells. Meanwhile, miRNAs can be regarded as key regulators in many biological processes, such as proliferation, apoptosis, and differentiation of cells<sup>11</sup>. MiRNAs are key participants in the osteogenic differentiation of BMSCs. For instance, Xie et al<sup>12</sup> have revealed that miR-181d inhibits the osteogenic differentiation of BMSCs by targeting Drosophila mothers against decapentaplegic protein 2 (Smad2), thus aggravating SONFH. MiR-27a<sup>13</sup> is capable of promoting the osteogenic differentiation and repressing the adipose differentiation of BMSCs by targeting PPARg and GREM1, thereby attenuating SONFH.

The aim of this study was to screen out differentially expressed miRNAs in BMSCs of SON-

FH patients. Moreover, we aimed to explore their effects on BMSCs and the possible underlying mechanisms.

#### **Patients and Methods**

#### General Data

This investigation was approved by the Ethics Committee of our hospital. Bone marrow tissues were collected from 5 patients with glucocorticoid (GC)-induced osteonecrosis of the femoral head (GC-ONFH, GC group) and 5 patients with secondary ONFH (control group) receiving total hip replacement in our hospital from July 2016 to August 2017. Inclusion criteria were as follows: patients aged 25-50 years old, without histories of smoking and heavy drinking. No patients had histories of hypertension, diabetes mellitus, hyperlipidemia, infectious diseases, and congenital diseases. Inclusion criteria for patients with GC-ONFH were as follows: patients with a GC intake of over 1600 mg or the use of GC as therapeutic drug for at least 4 weeks. Inclusion criteria for patients with secondary ONFH were: patients treated with GC previously.

### Separation and Culture of BMSCs

During total hip replacement, bone marrow tissues (5-10 mL) were removed from the proximal end of the femur using a sterile syringe. Collected tissues were immediately transferred to a sterile container and a super clean bench. In the super clean bench, bone marrow tissues were transferred to a centrifuge tube containing phosphate-buffered saline (PBS) solution and carefully pipetted using a pipette to make into cell suspension. Next, the cell suspension was transferred to a centrifuge tube containing an equal volume of leukocyte separation solution, followed by centrifugation at 2000 r/min for 30 min. After that, the mononuclear cell layer was taken and re-suspended in Dulbecco's Modified Eagle's Medium (DMEM; Gibco, Rockville, MD, USA) containing 10% fetal bovine serum (FBS; Gibco, Rockville, MD, USA). The cells were uniformly inoculated into 6-well plates and cultured in a 5% CO<sub>2</sub>, 37°C incubator under the humidity of 95%. The culture medium was replaced every 3 days.

# Detection of Surface Antigens Via Flow Cytometry

Flow cytometry was employed to identify cell phenotypes. First, the cells were digested with 0.25% trypsin, washed with PBS twice and

re-suspended in 500  $\mu L$  of PBS. Then, the cells were incubated with 5  $\mu L$  of cluster of differentiation 44 (CD44) antibody and 5  $\mu L$  of CD45 antibody for 30 min. Finally, a flow cytometer was used for loading and analysis, with 8,000 cells for each tube.

## Screening of Differential MiRNAs Through Gene Chip Method

High-throughput expression profile chip method was used to explore differentially expressed miRNAs between GC group and control group. Total RNAs were extracted from PC12 cells by TRIzol kit (Invitrogen, Carlsbad, CA, USA). Extracted RNA was quantified using a NanoDrop kit (Thermo Fisher Scientific, Waltham, MA, USA). The integrity of RNAs was assessed by Bioanalyzer 2100 (Agilent, Santa Clara, CA, USA). In this study, total RNA (100 ng) was used to prepare complimentary ribonucleic acids (cRNAs) in accordance with 3' IVT Express kit (Affymetrix, Santa Clara, CA, USA). Thereafter, cRNAs were hybridized on a Primeview Human array (Affymetrix, Santa Clara, CA, USA) at 45°C for 16 h according to the instructions of GeneChip 3' Array (Affymetrix, Santa Clara, CA, USA). In addition, the array was processed on a FS-450 fluid station (Affymetrix, Santa Clara, CA, USA) for washing and staining, followed by scanning using a GeneChip scanner (Affymetrix, Santa Clara, CA, USA). Raw data of CEL file were imported into the Partek Genomics Suite 6.6 software, and the probe set was normalized using the Robust Multiarray Average method. One-way analysis of variance (ANOVA) was adopted to determine the significance of differentially expressed genes, and p-value was corrected using false discovery rate (FDR).

#### Cell Experiment Protocols

MiR-15b mimics, miRNA control (miR-con), and miR-15b inhibitor were bought from Gene-Pharma Co., Ltd. (Shanghai, China).

Protocol for cell transfection: BMSCs were transfected with miR-15b mimics ( $10 \, \mu M$ ) and miR-15b inhibitor ( $10 \, \mu M$ ) using Lipofectamine  $2000^{TM}$  (Invitrogen, Carlsbad, CA, USA) for 6 h. After that, the medium containing transfection reagent was discarded. Next, BMSCs were cultured in fresh medium for 48 h for subsequent experiments.

Protocol for induction of osteogenic differentiation of cells: complete medium containing 10% FBS, 10 nmol/L dexamethasone, 10 mmol/L  $\beta$ -glycerophosphate, 50  $\mu$ g/mL ascorbic acid, 1%

penicillin-streptomycin, and 1% HEPES was utilized to induce cell osteogenic differentiation for 2 weeks.

In the first experiment, BMSCs from patients with GC-ONFH and secondary NOFH were divided into two groups, including control group and GC group. Quantitative Reverse-Transcription Polymerase Chain Reaction (qRT-PCR) assay was then conducted to detect the expression level of miR-15b in the two groups.

In the second experiment, cells in control group were divided into 2 groups, namely control group and miR-15b mimics treatment group [treated with miR-15b mimics (10  $\mu$ M)]. Then, the effect of miR-15b on the osteogenic differentiation of BMSCs was detected through alizarin red staining.

In the third experiment, all cells were divided into three groups, including control group, miR-15b mimics treatment group, and miR-15b inhibitor treatment group. The effect of miR-15b on the transforming growth factor beta (TGF-β) signaling pathway was determined *via* Western blotting.

## Alizarin Red Staining

After induction of osteogenic differentiation, the culture medium in each well was carefully aspirated. Subsequently, the cells were washed twice with PBS and fixed with 4 mL of neutral formalin for 30 min. After washing again with PBS twice, the cells were stained with 1 mL of alizarin red staining solution for 5 min. After that, the staining solution was aspirated, and the cells were washed twice with PBS solution. Finally, the cells were observed under a microscope and photographed.

#### Western Blotting

An appropriate amount of radioimmunoprecipitation assay (RIPA) was taken, added with protease inhibitor phenylmethanesulfonyl fluoride (PMSF) at a ratio of 100:1 and mixed to prepare cell lysis buffer (Beyotime, Shanghai, China). After trypsinization, the cells were collected and added with lysis buffer. The resulting product was collected and transferred to an Eppendorf (EP) tube (Hamburg, Germany), followed by centrifugation at 4°C and 14,000 rpm for 30 min by a low-temperature high-speed centrifuge. Subsequently, the protein supernatant was collected. Thereafter, the proteins were denatured at 95°C for 10 min via thermal bath. Prepared protein samples were stored in a refrigerator at -80°C for use. The concentration of extracted protein samples was determined by the bicinchoninic acid (BCA) kit (Pierce, Rockford, IL, USA). Protein samples were then separated by sodium dodecyl sulfate polyacrylamide gel electrophoresis (SDS-PAGE) at constant pressure (80 V) for 2.5 h and transferred onto polyvinylidene difluoride (PVDF) membranes using the semi-dry method (Roche, Basel, Switzerland). After that, the membranes were blocked in Tris-Buffered Saline with Tween®20 (TBST) buffer containing 5% skim milk powder for 1 h. Next, the membranes were incubated with primary antibodies, followed by rinsing with TBST solution for 3 times (10 min/time). Next, the membranes were incubated with corresponding secondary antibody at room temperature for 2 h and rinsed twice with TBST and once with TBS (10 min/time). Immuno-reactive bands were finally exposed by the enhanced chemiluminescence (ECL) method in the dark. The relative expression level of proteins was analyzed using the Adobe Photoshop software (Adobe, San Jose, CA, USA).

## **ORT-PCR** Assay

QRT-PCR was used to detect the expression of messenger RNA (mRNA) and miRNA in cells. Samples containing 500 ng of RNAs were divided into three groups, and total RNA in each group was diluted 10 times. 3 µL of total RNA was taken for PCR amplification. The amplification level of target genes was verified using 5% agarose gel electrophoresis. LabWorks 4.0 image acquisition and analysis software was applied for data quantitation and processing. For samples in each group, the assay was repeated for three times to obtain reliable data. Relative expression of target genes was calculated by the 2-DACT method. Primer sequences used in this study were shown in Table I.

## Luciferase Reporter Gene Assay

Bioinformatics software (TargetScan; http://www.targetscan.org/vert\_72/) was used to predict the possible targets of miR-15b. In this experiment, wild-type and mutant Smad7 were amplified and cloned into psiCHECKTM-2 luciferase plasmids (Promega, Madison, WI, USA) to generate wild-type and mutant reporter genes, respectively. HEK293 cells were cultured in 24-well plates and co-transfected with miR-15b mimics or miR-con and wild-type or mutant plasmids for 48 h. The activity of luciferase was finally detected using dual-luciferase reporter reagent (Promega, Madison, WI, USA).

### Statistical Analysis

Statistical Product and Service Solutions (SPSS) 20.0 software (IBM Corp., Armonk, NY, USA) was used for all statistical analysis. For each assay, 3 parallel groups or 3 replicates were set. Experimental results were expressed as mean  $\pm$  standard deviation (Mean  $\pm$  SD). The *t*-test was used to compare the difference between the two groups. One-way ANOVA was applied to compare the differences among different groups, followed by Post-Hoc Test (Least Significant Difference). p<0.05 suggested a statistical difference, and p<0.01 was considered statistically significant.

#### Results

## Differentially Expressed MiRNAs Screened

Differentially expressed miRNAs in serum between GC group and control group were screened by gene expression profile chip method. With Fold Change >3 and adjust p<0.001 as screening criteria, a total of 120 miRNAs were finally screened out. Among 120 differentially expressed circle RNAs, 57 were significantly up-regulated, and 63 were significantly down-regulated. Among them, 27 miRNAs displayed a difference of more than 10 times in the expression level, including 8 up-regulated miRNAs and 19 down-regulated miRNAs. Especially, miR-15b was one of those miRNAs with the most significant difference in the expression level (Figure 1).

#### Identification and Culture of BMSCs

After 5 d of primary culture, the number of red blood cells and other suspended cells was markedly reduced. The morphology of primary cultured BMSCs was shown in Figure 2A. Subsequently, two BMSC-specific markers were used to distinguish BMSCs from hemocytes and other monocytes. Flow cytometry showed that the proportion of CD44-positive cells in cultured BMSCs was 99.7%, while that of CD45-positive cells was only 0.17%. This implied that BMSCs exhibited rela-

Table I. Primer sequences.

Primer n	me Prime	er sequences (5'- 3')
MiR-15b		CACATCATGGTTTA-3' ATGTCTGCGTATCTC-3'
Smad7	5'-TGTCCA	GATGCTGCGTATCTC-3' CCTCCTCCCAGTATG-3'

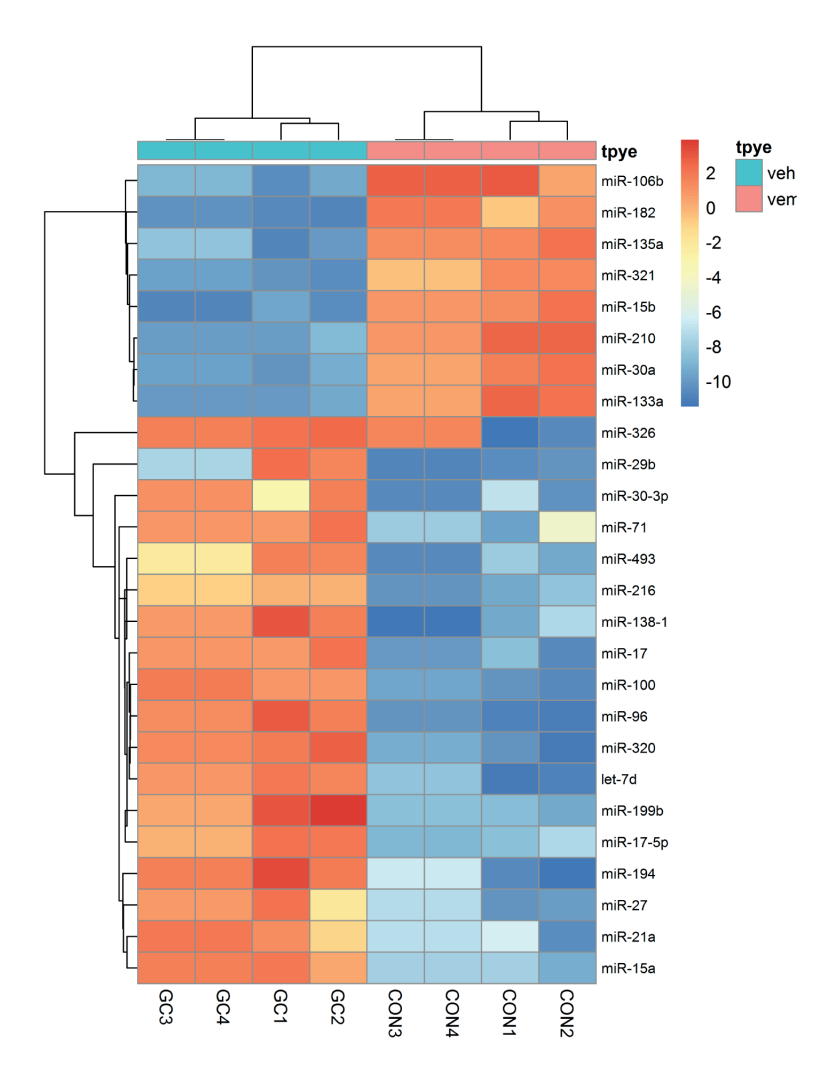


**Figure 1.** Differentially expressed miRNAs screened *via* gene expression profile chip method.

tively high purity and could be used for further experiment. QRT-PCR results revealed that the expression level of miR-15b was overtly lower in BMSCs of patients with GC-ONFH than that in patients with secondary ONFH (p<0.01; Figure 2B and 2C). These results suggested that the expression level of miR-15b might be correlated with GC-ONFH.

## Effects of GC on Osteogenic Differentiation Capacity of BMSCs and Expression Level of MiR-15b

BMSCs collected from patients with GC-ON-FH and those with secondary ONFH were cultured for osteogenic differentiation for 14 d. Alizarin red staining was performed to evaluate the osteogenic differentiation of cells in the two groups. The results uncovered that the osteogenic

differentiation capacity of BMSCs was remarkably enhanced in patients with GC-ONFH when compared with that in patients with secondary ONFH (Figure 3A). Subsequently, BMSCs collected from patients with secondary ONFH were treated with different concentrations of dexamethasone. QRT-PCR assay was then conducted to measure the expression level of miR-15b in cells. The results demonstrated that GC decreased the expression level of miR-15b in a dose-dependent manner, and the difference was statistically significant (*p*<0.01; Figure 3B).

# Effect of MiR-15b Expression on Osteogenic Differentiation of BMSCs

Compared with control group, the osteogenic differentiation ability of cells was overtly promoted in miR-15b mimic treatment group. These

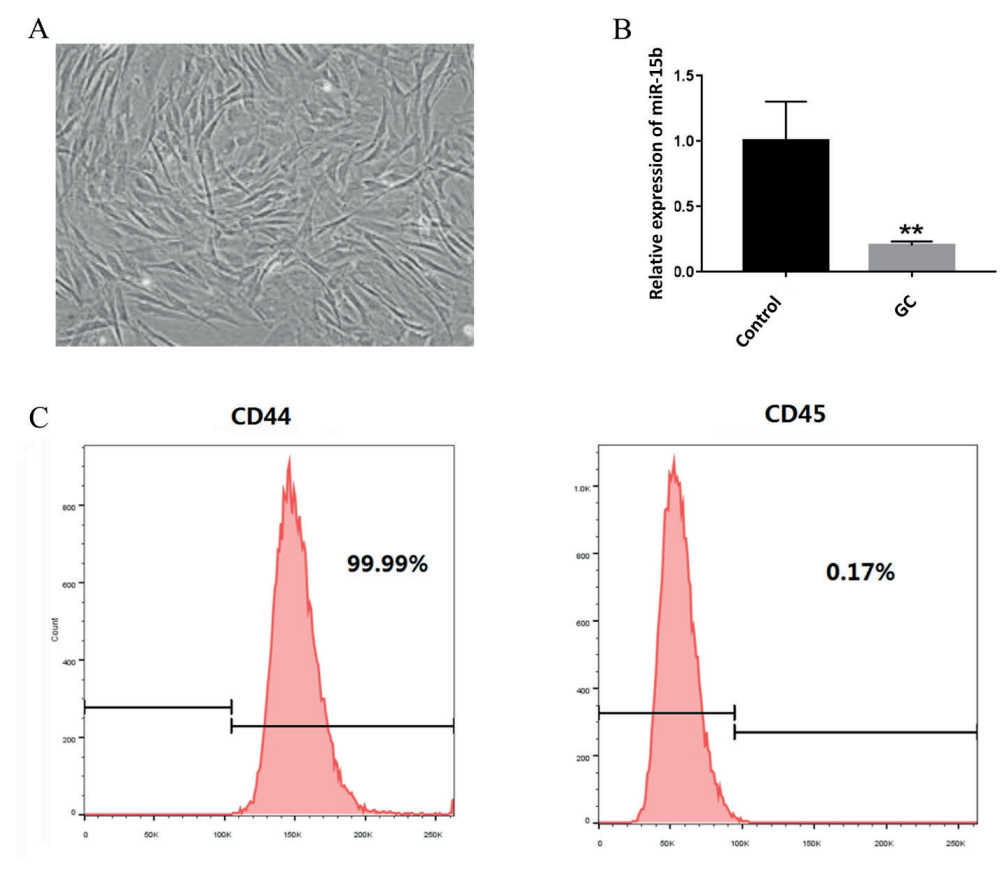


**Figure 2.** MiR-15b expression in BMSCs of patients with secondary ONFH and those with GC-ONFH, and morphology and identification of BMSCs. **A,** Difference in miR-15b expression in BMSCs between patients with secondary ONFH and those with GC-ONFH detected via qRT-PCR assay (magnification × 40), **B,** Morphology of BMSCs, and **C,** Surface antigens (CD44 and CD45) of BMSCs determined through flow cytometry.

findings suggested that miR-15b was a key participant in the osteogenic differentiation of BMSCs (Figure 4).

## Direct Targets of MiR-15b Predicted and Verified

Bioinformatics software (TargetScan) predicted that Smad7 might be a potential target of miR-15b (Figure 5A). To further confirm the interaction between miR-15b and Smad7, luciferase reporter assay was employed to detect the response of wild-type and mutant Smad7 to miR-15b and miR-con in HEK293 cells, respectively (Figure 5B). The results showed that the fluorescence response intensity decreased significantly in HEK293 cells with wild-type Smad7 transfected with miR-15b. However, no evident changes were observed in HEK293 cells with mutant Smad7 (Figure 5C). QRT-PCR and Western blotting assays were performed for further verification. The results indicated that transfection of miR-15b mimics sig-

nificantly reduced the mRNA and protein levels of Smad7. However, knockdown of miR-15b elevated the expression level of Smad7 (Figure 5D and 5E). In summary, these results indicated that miR-15b negatively modulated the expression of Smad7 by binding to the 3'-untranslated region (3'-UTR) of Smad7.

## Effect of MiR-15b on TGF- $\beta$ Signaling Pathway

MiR-15b mimics treatment group exhibited markedly down-regulated protein expression level of Smad7 and up-regulated expression level of phosphorylated (p)-Smad2/3 in comparison with control group, and the differences were statistically significant (p<0.01). Conversely, miR-15b inhibitor treatment group exhibited significantly up-regulated protein expression level of Smad7 and down-regulated expression level of p-Smad2/3 in comparison with control group, showing statistically significant differences (p<0.01). Compared

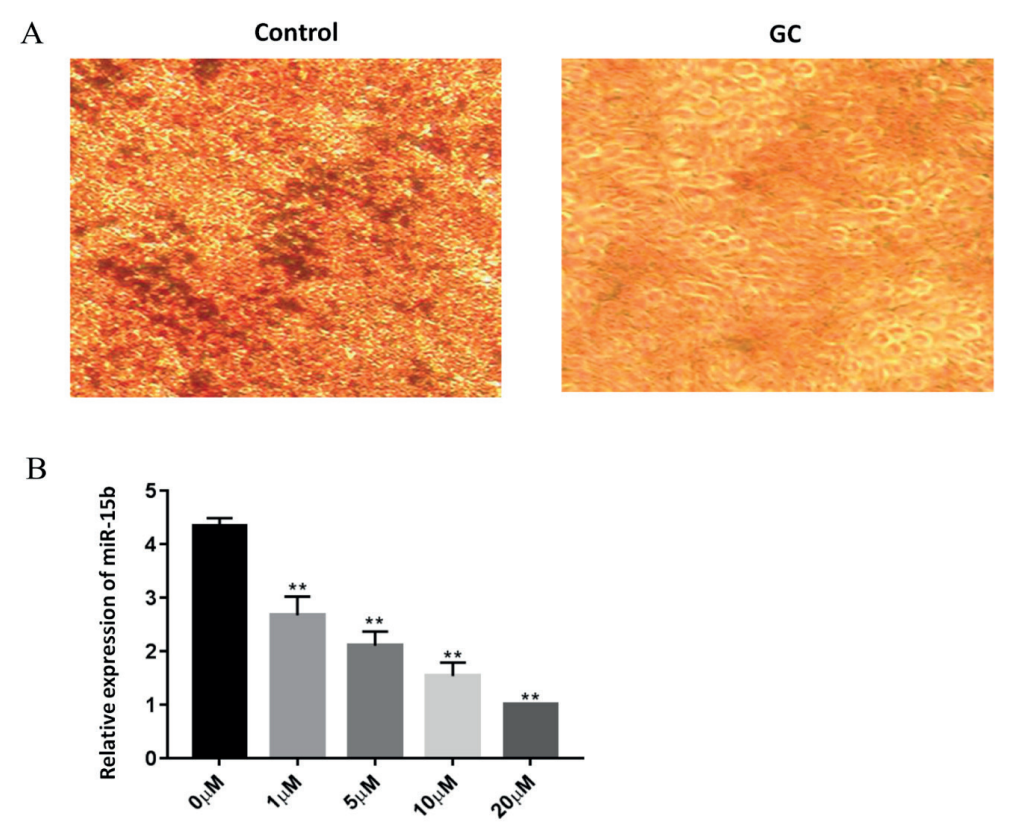


**Figure 3.** Effects of GC on osteogenic differentiation capacity of BMSCs and expression level of miR-15b. **A,** Effect of GC on osteogenic differentiation ability of BMSCs detected through alizarin red staining (magnification × 40), **B,** Effect of GC on expression level of miR-15b in BMSCs.

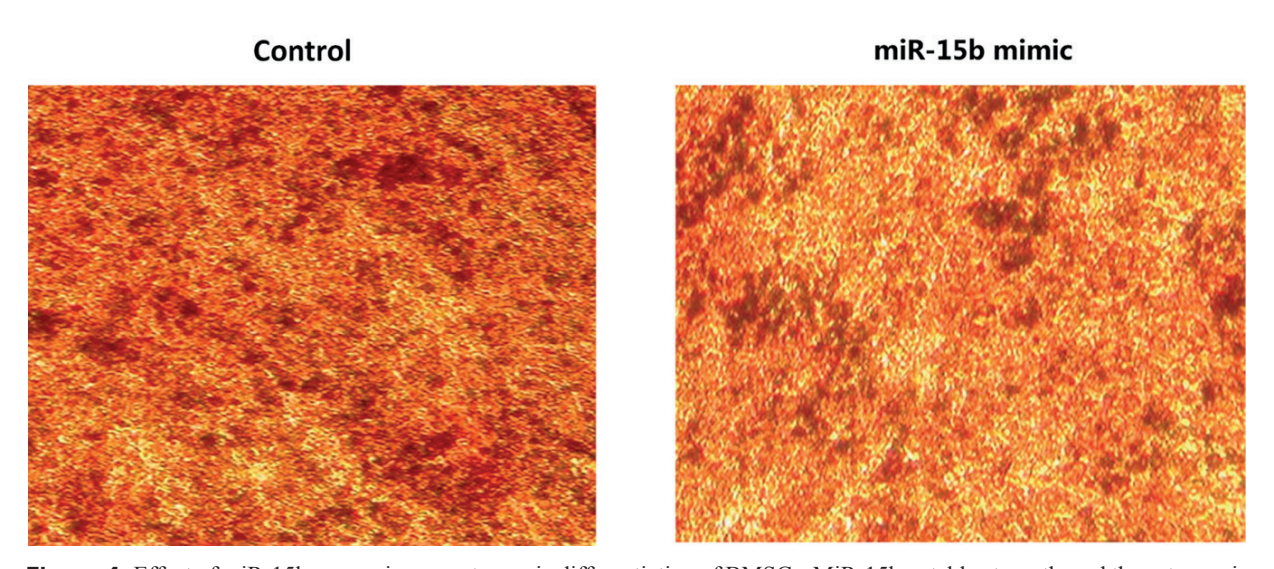
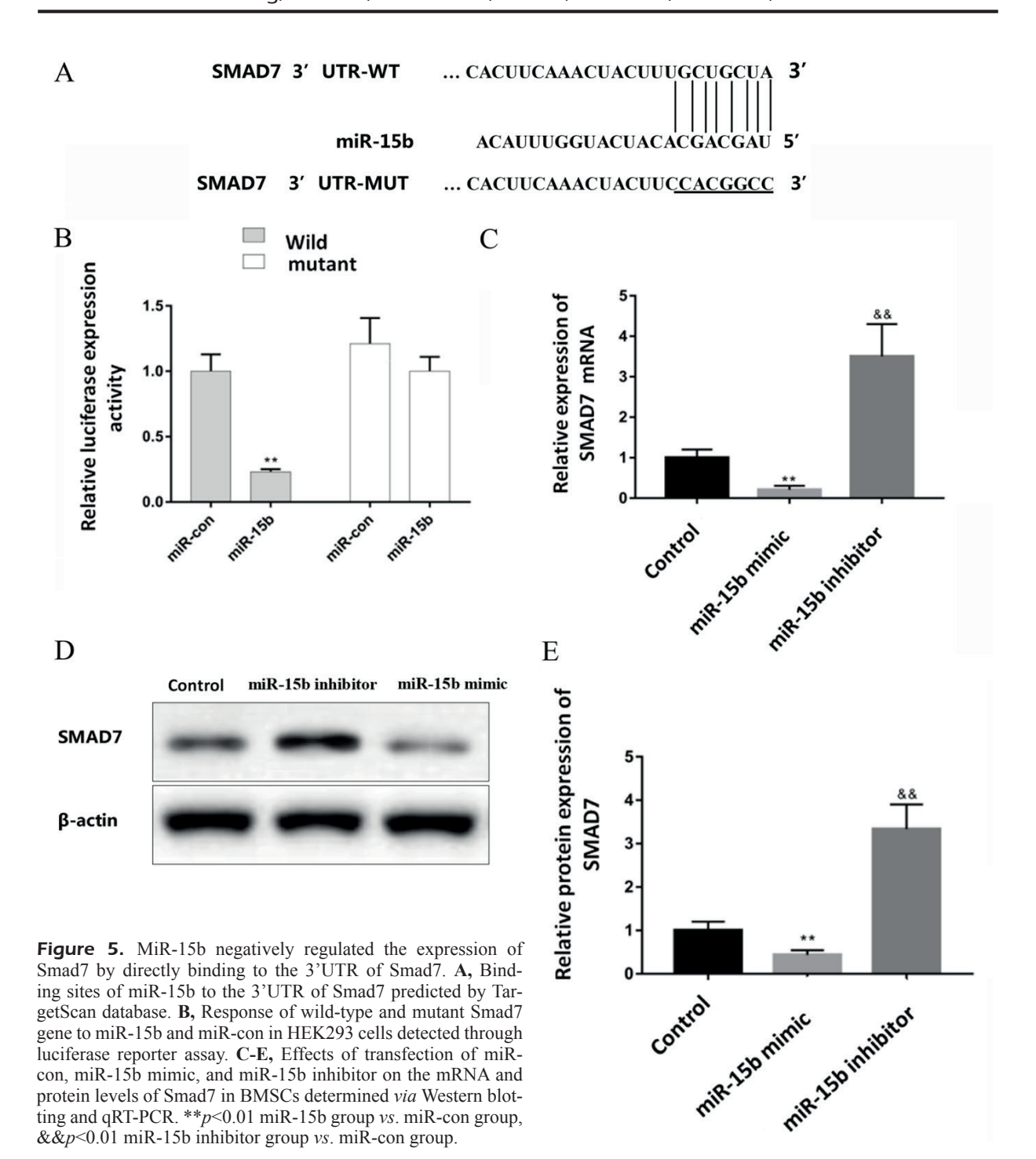


**Figure 4.** Effect of miR-15b expression on osteogenic differentiation of BMSCs. MiR-15b notably strengthened the osteogenic differentiation capacity of BMSCs (magnification × 40).

with control group, the mRNA expression level of Runx2 increased evidently in cells of miR-15b mimics treatment group, while decreased distinct-

ly in cells of miR-15b inhibitor treatment group, displaying statistically significant differences (Figure 6).



### Discussion

As cells with strong proliferative capacity and multi-directional differentiation potential, BM-SCs have important physiological and pathological effects in the development and progression of various diseases. Current studies have found that they can differentiate into various bone stromal

cells. Therefore, BMSCs play crucial roles in the treatment of ONFH. Furthermore, their ability to differentiate into bone cells and mechanism of action are of great significance in the pathogenesis of SONFH<sup>14</sup>.

In the present research, flow cytometry indicated that the proportion of CD44-positive cells in BM-SCs cultured was 99.7%, while that of CD45-posi-

tive cells was only 0.17%. This implied that BMSCs had relatively high purity. Subsequently, differentially expressed miRNAs in serum between GC group and control group were screened via gene expression profile chip method. Totally 120 miR-NAs were screened out, with Fold Change >3 and adjust p<0.001 as screening criteria. Among 120 differentially expressed circle RNAs, 57 were significantly up-regulated, while 63 were down-regulated. The difference in the expression level of 27 miRNAs was over 10 times. Among them, the expression level of 8 miRNAs increased, while that of 19 miRNAs declined. Especially, miR-15b was one of the miRNAs with the most significant difference in the expression level. Subsequently, qRT-PCR assay was carried out to further verify the results of

high-throughput transcriptome. It was discovered that the expression level of miR-15b declined significantly in BMSCs of patients with GC-ONFH when compared with that in patients with secondary ONFH (p<0.01). Alizarin red staining was conducted to detect the degree of osteogenic differentiation of cells in the two groups after 14 d of osteogenic differentiation induction. This might help to confirm the effect of miR-15b expression on the osteogenic differentiation of BMSCs. The results manifested that the osteogenic differentiation ability of BMSCs was prominently stronger in GC group than that of control group. Thereafter, BMSCs were treated with different concentrations of dexamethasone to determine the effect of GC treatment on miR-15b. QRT-PCR assay revealed

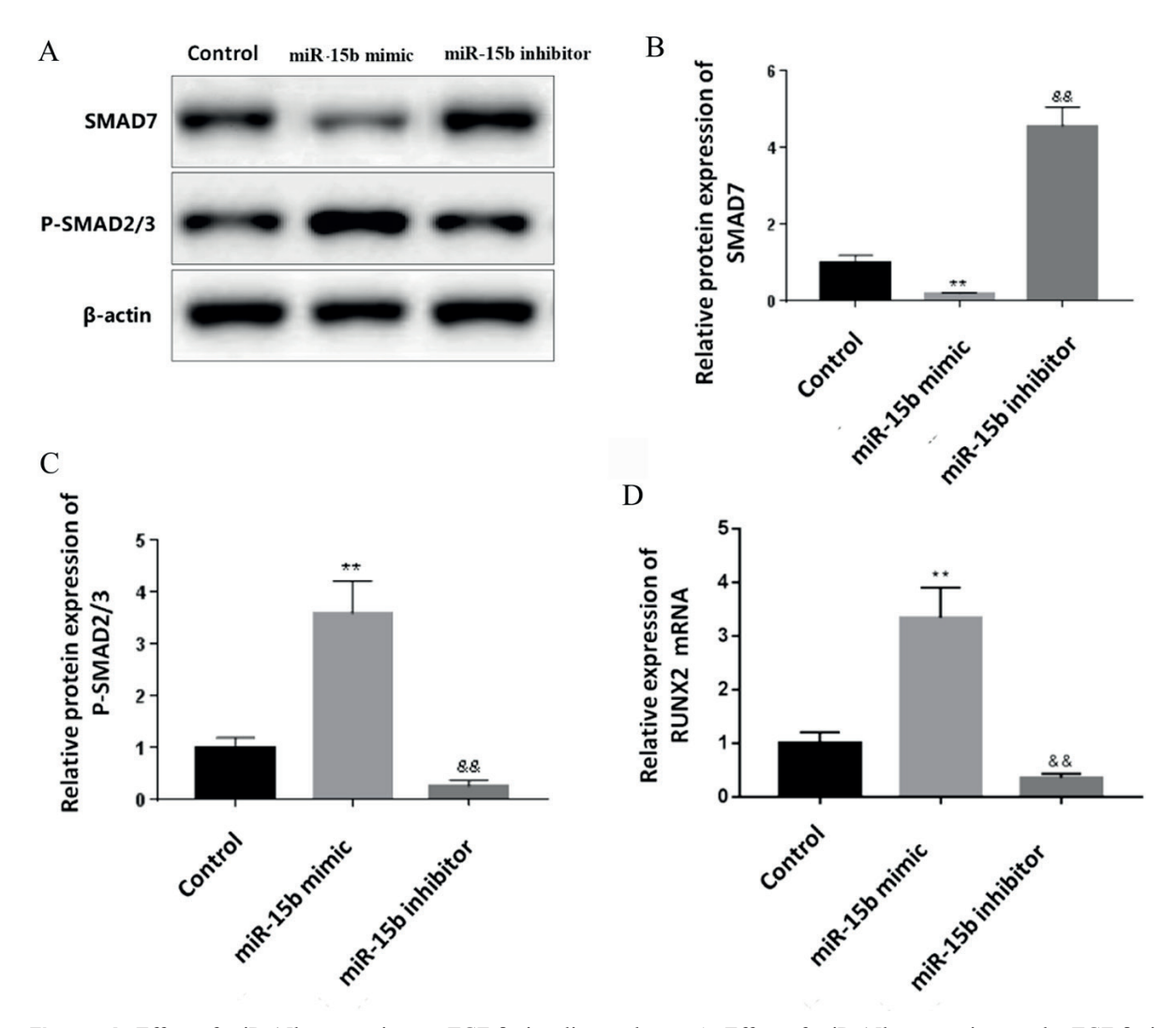


**Figure 6.** Effect of miR-15b expression on TGF-β signaling pathway. **A,** Effect of miR-15b expression on the TGF-β signaling pathway determined via Western blotting. **B,** Relative protein expression of SMAD7. **C,** Relative protein expression of p-SMAD2/3. **D,** Effect of miR-15b on the expression level of Runx2 detected through qRT-PCR assay.

that dexamethasone reduced the expression level of miR-15b in a dose-dependent manner. To verify the effect of miR-15b on osteogenic differentiation, miR-15b mimics were transfected into BMSCs in control group. It was suggested that compared with control group, the osteogenic differentiation ability was remarkably enhanced in miR-15b mimic treatment group. To study the potential mechanism of miR-15b on BMSCs, bioinformatics software (TargetScan) was used for prediction. The results found that Smad7 might be a potential target of miR-15b. Subsequent luciferase reporter gene assay validated that Smad7 was a direct target of miR-15b. In comparison with control group, miR-15b mimics treatment group exhibited significantly down-regulated protein expression level of Smad7 and up-regulated protein expression level of p-Smad2/3 in cells. Compared with control group, the protein expression level of Smad7 in cells was evidently reduced, while the expression level of p-Smad2/3 was prominently elevated in cells of miR-15b mimic treatment group, and the differences were statistically significant (p<0.01). The above two indexes showed the opposite tendencies in miR-15b inhibitor treatment group, with statistically significant differences (p<0.01). Compared with control group, the expression level of Runx2 was markedly up-regulated in cells of miR-15b mimics treatment group, while down-regulated in miR-15b inhibitor treatment group.

Sun et al<sup>15</sup> have demonstrated that the TGF-B signaling pathway plays a vital role in the osteogenic differentiation of BMSCs. TGF-β binds to membrane receptors [TGF-β receptor II (TβRII) and ALK5/TβRI] to activate the Smad signaling pathway. Ultimately, this may lead to increased expression level of Runx2, which is a transcription factor regulated by Smad. Furthermore, this can regulate the osteogenic differentiation of BMSCs<sup>16</sup>. Smad7, an inhibitory Smad protein, is able to suppress the phosphorylation of Smad2/3 protein by binding to TBRI. Meanwhile, it can also recruit Smurf1/2, thereby giving rise to the ubiquitination and degradation of TBRI. Eventually, this may result in the repression of the TGF-β signaling pathway<sup>17</sup>.

### Conclusions

This study demonstrated that miR-15b was lowly expressed in BMSCs of patients with GC-ONFH, significantly up-regulating the pro-

tein expression of Smad7 and inhibiting TGF- $\beta$  signaling pathway. Ultimately, this could result in weakened osteogenic differentiation ability of BMSCs.

#### **Funding Acknowledgements**

Fujian Provincial Department of Finance Special Allocation (2018B022, BPB-LJH2015-2); The Youth Backbone Talent Training Program of Fujian Provincial Health System (2017-ZQN-48); 2018 '13th Five-Year plan' project of Fujian Provincial Department of Education (FJJKCG18-021); Startup Fund for Scientific Research, Fujian Medical University (2017XQ1075); Fujian Provincial Department of Health Youth Fund Project (2016-2-17).

#### **Conflict of Interests**

The Authors declare that they have no conflict of interests.

#### References

- Asano T, Takahashi KA, Fujioka M, Inoue S, Okamoto M, Sugioka N, Nishino H, Tanaka T, Hirota Y, Kubo T. ABCB1 C3435T and G2677T/A polymorphism decreased the risk for steroid-induced osteonecrosis of the femoral head after kidney transplantation. Pharmacogenetics 2003; 13: 675-682.
- FANG S, LI Y, CHEN P. Osteogenic effect of bone marrow mesenchymal stem cell-derived exosomes on steroid-induced osteonecrosis of the femoral head. Drug Des Devel Ther 2018; 13: 45-55.
- Kubo T, Ueshima K, Saito M, Ishida M, Arai Y, Fujiwara H. Clinical and basic research on steroid-induced osteonecrosis of the femoral head in Japan. J Orthop Sci 2016; 21: 407-413.
- POUYA F, KERACHIAN MA. Avascular necrosis of the femoral head: are any genes involved? Arch Bone Jt Surg 2015; 3: 149-155.
- PHIPPS MC, HUANG Y, YAMAGUCHI R, KAMIYA N, ADAPALA NS, TANG L, KIM HK. In vivo monitoring of activated macrophages and neutrophils in response to ischemic osteonecrosis in a mouse model. J Orthop Res 2016; 34: 307-313.
- 6) LIU X, LI Q, NIU X, HU B, CHEN S, SONG W, DING J, ZHANG C, WANG Y. Exosomes secreted from human-induced pluripotent stem cell-derived mesenchymal stem cells prevent osteonecrosis of the femoral head by promoting angiogenesis. Int J Biol Sci 2017; 13: 232-244.
- 7) Mont MA, Cherian JJ, Sierra RJ, Jones LC, Lieberman JR. Nontraumatic osteonecrosis of the femoral head: where do we stand today? A ten-year update. J Bone Joint Surg Am 2015; 97: 1604-1627.
- SEN RK, TRIPATHY SK, AGGARWAL S, MARWAHA N, SHARMA RR, KHANDELWAL N. Early results of core decompression and autologous bone marrow mononuclear cells instillation in femoral head osteonecrosis: a randomized control study. J Arthroplasty 2012; 27: 679-686.

- RAWADI G, VAYSSIERE B, DUNN F, BARON R, ROMAN-ROMAN S. BMP-2 controls alkaline phosphatase expression and osteoblast mineralization by a Wnt autocrine loop. J Bone Miner Res 2003; 18: 1842-1853.
- 10) TAN G, KANG PD, PEI FX. Glucocorticoids affect the metabolism of bone marrow stromal cells and lead to osteonecrosis of the femoral head: a review. Chin Med J (Engl) 2012; 125: 134-139.
- 11) LIU G, LUO G, BO Z, LIANG X, HUANG J, LI D. Impaired osteogenic differentiation associated with connexin43/microRNA-206 in steroid-induced avascular necrosis of the femoral head. Exp Mol Pathol 2016; 101: 89-99.
- XIE Y, Hu JZ, SHI ZY. MiR-181d promotes steroidinduced osteonecrosis of the femoral head by targeting SMAD3 to inhibit osteogenic differentiation of hBMSCs. Eur Rev Med Pharmacol Sci 2018; 22: 4053-4062.
- 13) Gu C, Xu Y, Zhang S, Guan H, Song S, Wang X, Wang Y, Li Y, Zhao G. MiR-27a attenuates adipogenesis and promotes osteogenesis in steroid-induced rat

- BMSCs by targeting PPARγ and GREM1. Sci Rep 2016; 6: 38491.
- 14) Wang A, Ren M, Wang J. The pathogenesis of steroid-induced osteonecrosis of the femoral head: a systematic review of the literature. Gene 2018; 671: 103-109.
- 15) Sun BY, Zhao BX, Zhu JY, Sun ZP, Shi YA, Huang F. Role of TGFbeta1 expressed in bone marrowderived mesenchymal stem cells in promoting bone formation in a rabbit femoral defect model. Int J Mol Med 2018; 42: 897-904.
- MAHBOUDI H, KAZEMI B, SOLEIMANI M, HANAEE-AHVAZ H, GHANBARIAN H, BANDEHPOUR M, ENDERAMI SE, KEHTARI M, BARATI G. Enhanced chondrogenesis of human bone marrow mesenchymal Stem Cell (BMSC) on nanofiber-based polyethersulfone (PES) scaffold. Gene 2018; 643: 98-106.
- 17) Hu BT, CHEN WZ. MOTS-c improves osteoporosis by promoting osteogenic differentiation of bone marrow mesenchymal stem cells via TGF-beta/ Smad pathway. Eur Rev Med Pharmacol Sci 2018; 22: 7156-7163.